Online Appendix for

# The Quanto Theory of Exchange Rates

Lukas Kremens Ian Martin

## IA.A Binary forecast accuracy

In this section, we follow the approach of Jordà and Taylor (2012) by computing a *correct classification frontier* (CCF) to assess the forecast performance of the quanto theory.

Denote by $f^Q_{i,j,t} = \text{QRP}_{i,t} - \text{QRP}_{j,t}$ and $f^B_{i,j,t}$ the forecasts obtained, respectively, from the quanto variable and a competitor benchmark for currency pair $(i, j)$ at time $t$. Similarly, $r_{i,t} = e_{i,t+1}/e_{i,t} - R^\$_t/R^i_t$ denotes the realized excess return of currency $i$ against the dollar, and $r_{i,j,t} = r_{i,t} - r_{j,t}$ represents the dollar-neutral return in currency pair $(i, j)$. We calculate the *true positive* (TP) and *true negative* (TN) rates for each forecasting model as a function of a threshold, $c$. For the quanto forecast, for instance,

$$\text{TP}(c) = \frac{\sum_{i,j\colon f^m_{i,j,t}>c \text{ and } r_{i,j,t}>0} 1}{\sum_{i,j\colon r_{i,j,t}>0} 1} \qquad \text{and} \qquad \text{TN}(c) = \frac{\sum_{i,j\colon f^Q_{i,j,t}<c \text{ and } r_{i,j,t}<0} 1}{\sum_{i,j\colon r_{i,j,t}<0} 1}.$$

These represent, respectively, the fractions of ex post positive long and short returns that were correctly identified ex ante as profitable by the forecasting model. For the same 55 dollar-neutral currency pairs used above, we find that $\text{TP}(0) = 0.50$, $\text{TN}(0) = 0.64$, with a weighted average correct classification of 0.57 for the quanto forecast.

As binary accuracy does not reflect the magnitudes of returns from the signal, we follow Jordà and Taylor (2012) and compute the corresponding *return-weighted* true positive ($\text{TP}^*$) and true negative ($\text{TN}^*$) rates as

$$\text{TP}^*(c) = \frac{\sum_{i,j\colon f^Q_{i,j,t}>c \text{ and } r_{i,j,t}>0} r_{i,j,t}}{\sum_{i,j\colon r_{i,j,t}>0} r_{i,j,t}} \qquad \text{and} \qquad \text{TN}^*(c) = \frac{\sum_{i,j\colon f^Q_{i,j,t}<c \text{ and } r_{i,j,t}<0} r_{i,j,t}}{\sum_{i,j\colon r_{i,j,t}<0} r_{i,j,t}}.$$

We find $\text{TP}^*(0) = 0.58$, $\text{TN}^*(0) = 0.67$, with a weighted average of 0.63. Both rates increase relative to the equally-weighted classifications, which implies that the direction

of excess return realizations is more likely to have been predicted by the quanto variable when these realizations are large.

The CCF (and analogously CCF$^*$) is defined as the set of pairs $\{\text{TP}(c), \text{TN}(c)\}$ for all possible values of $c$ between $-\infty$ and $\infty$. Varying the threshold level, $c$, trades off true positives against true negatives by shifting the direction of the forecast. For instance, for $c = \infty$, the true negative rate is maximized at TN $= 1$, at the cost of TP $= 0$. Since TN$(c)$ and TP$(c)$ must lie between 0 and 1, we can plot the resulting CCF in the unit square, and compute the *area under the CCF* (AUC). Intuitively, the AUC can be interpreted as the probability that the forecast for a randomly chosen positive return realization will be higher than that for a randomly chosen negative return realization. Under the UIP forecast the excess return on any currency is 0, so the CCF is the diagonal with slope $-1$ in the unit square and, accordingly, AUC $= 0.5$.

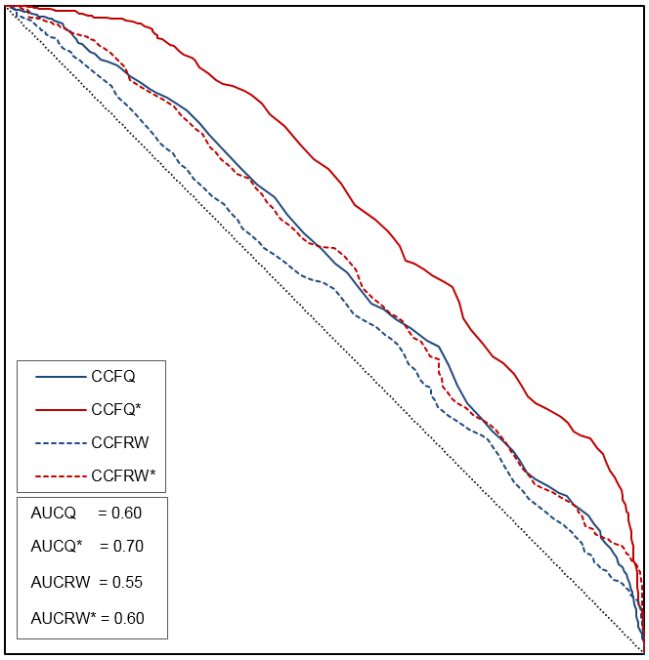


Figure IA.1: Correct classification frontier (CCF) and AUC statistics for the quanto excess return forecast, and a competitor excess return forecast under which exchange rates follow a random walk.

We benchmark the quanto forecast against the driftless random walk model considered above (which forecasts the currency excess return as being equal to the interest rate differential). Figure IA.1 shows the resulting CCFs. The quanto forecast outperforms the random walk model for equally-weighted and return-weighted classifications. For the quanto forecast, AUCQ $= 0.60$ and AUCQ$^*$ $= 0.70$, while the random walk

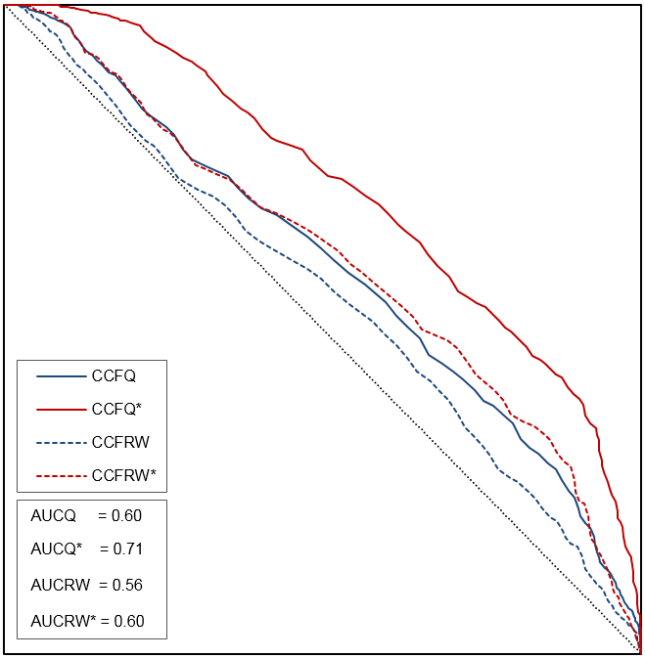


Figure IA.2: Reverse-conditioned correct classification frontier (CCF) and AUC statistics for the quanto excess return forecast, and a competitor excess return forecast under which exchange rates follow a random walk.

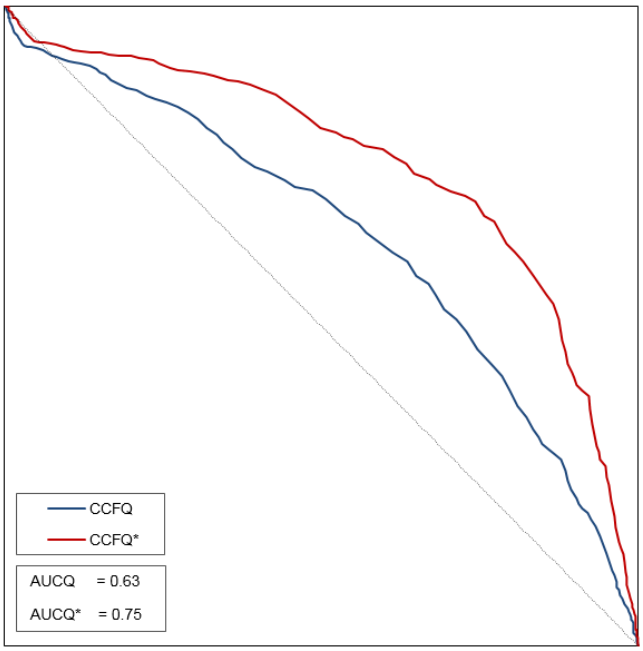


Figure IA.3: Correct classification frontier (CCF) and AUC statistics for forecasts of currency appreciation.

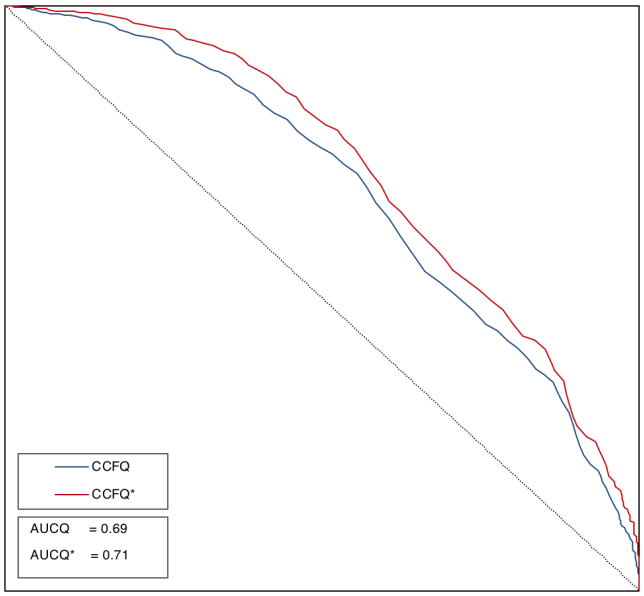


Figure IA.4: Reverse-conditioned correct classification frontier (CCF) and AUC statistics for forecasts of currency appreciation.

model achieves AUCRW = 0.55 and AUCRW$^*$ = 0.60. Both forecasts correctly identify large returns more often than small returns, as the CCF$^*$ (red) lies above the CCF (blue) in both cases.

We also reverse the conditioning in the true positive and true negative rates, to calculate how likely a forecast is to signal the correct direction of trade, and denote these by PT($c$) and NT($c$), respectively. In the case of the quanto theory,

$$\text{PT}(c) = \frac{\sum_{i,j:\, f^Q_{i,j,t}>0 \text{ and } r_{i,j,t}>c} 1}{\sum_{i,j:\, f^Q_{i,j,t}>0} 1} \qquad \text{and} \qquad \text{NT}(c) = \frac{\sum_{i,j:\, f^Q_{i,j,t}<0 \text{ and } r_{i,j,t}<c} 1}{\sum_{i,j:\, f^Q_{i,j,t}<0} 1}.$$

We find PT(0) = 0.60, NT(0) = 0.54, PT$^*$(0) = 0.65, and NT$^*$(0) = 0.63. Plotting the resulting CCFs, Figure IA.2 shows that the quanto variable outperforms the random walk forecast with AUC measures of AUCQ = 0.60 and AUCQ$^*$ = 0.71, as against the random walk model with AUCRW = 0.55 and AUCRW$^*$ = 0.60.

Figures IA.3 and IA.4 repeat this exercise, but now the goal is to forecast currency appreciation, as opposed to currency excess returns. In this case, the random walk forecast is represented by the diagonal with slope $-1$ in the unit square, and AUC = 0.5. As the figures show, the quanto forecast outperforms the random walk model, with AUCQ = 0.63 and AUCQ$^*$ = 0.75. The outperformance persists under reverse

conditioning, with AUCQ = 0.69 and AUCQ$^*$ = 0.71.

# IA.B Quantos in Colacito and Croce (2011)

This section studies the relationship between the currency risk premium, QRP, and the residual covariance term in the two-country long-run risk model of Colacito and Croce (2011). Log consumption growth, log dividend growth, the long-run risk variable, the log SDF, the log market return, and the log risk-free rate follow these processes:

$$\begin{aligned}
\Delta c_t &= \mu_c + x_{t-1} + \varepsilon_{c,t}, \\
\Delta d_t &= \mu_d + \lambda x_{t-1} + \varepsilon_{d,t}, \\
x_t &= \rho x_{t-1} + \varepsilon_{x,t}, \\
m_{t+1} &= \log\delta - \psi^{-1} x_t + \kappa_c \frac{1-\gamma\psi}{\psi(1-\rho\kappa_c)} \varepsilon_{x,t+1} - \gamma\varepsilon_{c,t+1}, \\
r_{d,t+1} &= \overline{r}_d + \psi^{-1} x_t + \kappa_d \frac{\lambda - 1/\psi}{1-\rho\kappa_d} \varepsilon_{x,t+1} + \varepsilon_{d,t+1}, \\
r_f &= \overline{r}_f + \psi^{-1} x_t.
\end{aligned}$$

The representative agent has Epstein–Zin preferences with risk aversion $\gamma$ and elasticity of intertemporal substitution $\psi$. Shocks are i.i.d. Normal over time, with mean zero and (diagonal) covariance matrix $\Sigma$, with diagonal $[\sigma^2, \varphi_d^2\sigma^2, \varphi_x^2\sigma^2]$. Thus returns and the SDF are jointly lognormal and subject to the issues described in Section 2.4. Between-country correlations of shocks are $\rho_c^{hf}$, $\rho_d^{hf}$, and $\rho_x^{hf}$, respectively. The exchange rate satisfies $e_{t+1}/e_t = M_{t+1}^f / M_{t+1}$, where $M^f$ denotes the foreign SDF (which is uniquely determined, as markets are complete).

The baseline calibration is symmetric, so both currencies are equally "risky." To generate a currency risk premium, we vary—one-by-one—the parameter values for (i) the volatility of the foreign long-run risk shock, governed by $\varphi_x^f$, (ii) its persistence, $\rho^f$, (iii) the cross-country correlation of long-run risk shocks, $\rho_x^{hf}$, and (iv) the cross-country correlation of consumption shocks, $\rho_c^{hf}$. We plot the resulting comparative statics in Figure IA.5 below. We use the baseline calibration of Colacito and Croce (2011) for all other model parameters. With the exception of $\rho_x^{hf}$, which is equal to 1 in the baseline calibration, we vary the parameters of interest in a symmetric window around their baseline values.

Through the lens of this model, we now consider the identity (6), which decomposes the currency risk premium into risk-neutral covariance (QRP) and the residual covariance term:

$$\mathbb{E}_t \frac{e_{i,t+1}}{e_{i,t}} - \frac{R^{\$}_{f,t}}{R^{i}_{f,t}} = \mathrm{QRP}_{i,t} - \underbrace{\mathrm{cov}_t \left( M_{t+1} R_{t+1}, \frac{e_{i,t+1}}{e_{i,t}} \right)}_{\text{residual covariance term}}.$$

As shown in panel (a), a lower long-run risk volatility generates a positive risk premium on the foreign currency, positive QRP, a positive residual, and a negative interest rate differential. (The calibration is monthly, but we annualize by multiplying all quantities by 12, so the $y$-axis is in annual terms in all four panels.) As the residual scales with QRP, we would expect to find that the coefficient on QRP in a forecasting regression is larger than 1. Qualitatively, the same holds for a lower persistence of the foreign long-run risk process in panel (b). The risk premia in panels (c) and (d) are symmetric, in the sense that they increase the expected appreciation of *both* currencies in another manifestation of Siegel's paradox (see Section 1.2). In the case of a less-than-perfect cross-country correlation of long-run risk shocks, the resulting risk premium is captured proportionately by QRP and the residual, and would lead to a $\beta$ coefficient larger than 1 in our forecasting regressions.

# IA.C Evidence from other quanto contracts

Due to the limited availability of time-series data on quanto forwards, we look at USD-denominated futures on the Nikkei 225 index, which have started trading on the CME prior to the beginning of our OTC sample. We collect prices for USD-denominated Nikkei 225 futures traded on CME, and JPY-denominated Nikkei 225 futures traded on JPX (Osaka) for a sample period from 2004 through 2017. (JPY-denominated futures are also traded on CME, but at much lower volumes than the JPX-traded contracts.) Contracts expire each quarter, in March, June, September, and December, and we use contracts with the latest available expiration, which have a maturity ranging from 9-12 months. To calculate the QRP and IRD measures, we use dollar- and yen-denominated LIBOR rates matched to the maturity of the respective pair of futures.

Table IA.1 below reports the results for our baseline regressions.

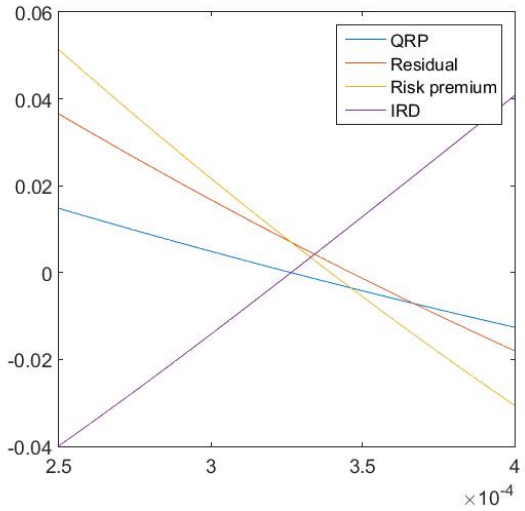


(a) Long-run risk volatility, $\varphi_x^f \sigma^f$

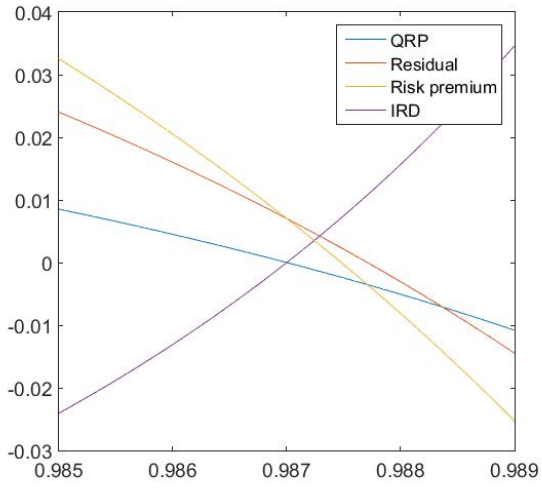


(b) Long-run risk persistence, $\rho^f$

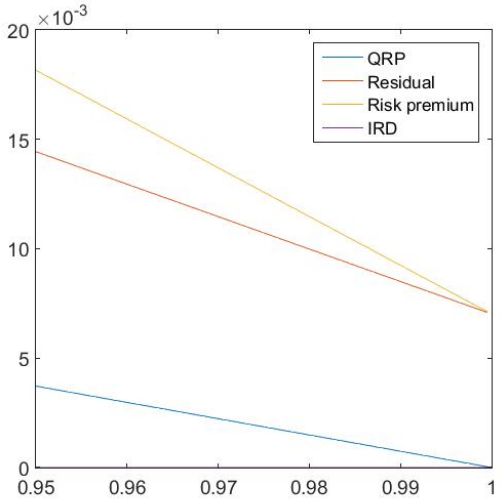


(c) Long-run risk cross-country correlation, $\rho_x^{hf}$

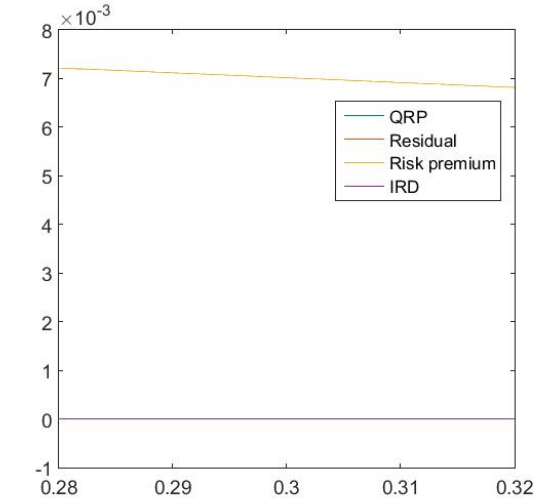


(d) Consumption risk cross-country correlation, $\rho_c^{hf}$

Figure IA.5: Each panel plots the comparative statics of the risk premium, risk-neutral covariance (QRP), the residual covariance, and the interest rate differential (IRD) with respect to a single model parameter (varied on the horizontal axis). In panel (d), QRP and IRD are both zero so the risk premium coincides with the residual.

Table IA.1: Forecasting regressions with exchange traded quanto-futures

This table reports the results of running regressions (20), (21), (22), and (24) for the USD/JPY currency pair at the 12-month horizon, based on dollar-denominated quanto futures on the Nikkei 225 (traded on CME). Since this setting essentially takes the perspective of a log investor who holds the Nikkei, the exchange rate is defined as ¥1 = \$$e$. We report the OLS estimates along with Hansen–Hodrick standard errors. $R^2$ are reported in %.

| Regression | (20) | (21) | (22) | (24) |
|---|---|---|---|---|
| $\alpha$ (p.a.) | 0.018 | 0.026 | 0.022 | 0.026 |
| | (0.027) | (0.036) | (0.036) | (0.036) |
| $\beta$ | 0.339 | 0.366 | 0.274 | 1.366 |
| | (0.720) | (1.917) | (0.587) | (1.917) |
| $\gamma$ | | | 1.293 | 1.366 |
| | | | (1.912) | (1.917) |
| $R^2$ | 0.26 | 0.26 | 3.60 | 3.44 |

We also calculate the out-of-sample $R^2$ based on mean-squared forecast errors as in Section 3. The quanto-based forecast outperforms the random walk and the UIP forecast by 1.96% and 3.25%, respectively, over the given period.

There are two important caveats. First, the available futures only provide information about a single currency-pair, dollar-yen. One of the strengths of the quanto data used in this paper lies in the cross-sectional dimension, which allows us to compute dollar-neutral forecasts in isolation from any base-currency effects. Table IA.5 suggests that the yen is not representative of the remaining panel. (USD-denominated futures on the FTSE 100 are also traded on the CME, which would provide information about dollar-sterling, but these contracts have only been traded since late 2015.) Second, the theory calls for quanto forward prices rather than quanto futures prices. If interest-rate movements are correlated with the underlying assets (as is plausibly true both of exchange rates and of the Nikkei 225) the two will differ. It is not clear how the pricing discrepancies between futures and forwards would affect the predictive power of our theory when applied to futures contracts.

# IA.D Supplementary Tables and Figures

Table IA.2: Principal components analysis of residuals

This table reports the loadings on the principal components of realized residuals obtained from the quanto theory (top panel) and the fixed-effects specification of regression (20) (bottom panel). In order to limit the impact of missing observations, the residuals are only obtained for the balanced panel of currencies (excluding DKK, KRW, and PLN).

| | **PC1** | **PC2** | **PC3** | **PC4** | **PC5** | **PC6** | **PC7** | **PC8** |
|---|---|---|---|---|---|---|---|---|
| | | | | *Theory residuals* | | | | |
| **AUD** | 0.520 | 0.160 | 0.108 | −0.443 | −0.273 | 0.235 | 0.578 | −0.183 |
| **CAD** | 0.311 | −0.015 | −0.107 | −0.257 | −0.090 | 0.458 | −0.490 | 0.606 |
| **CHF** | 0.194 | −0.124 | 0.644 | 0.344 | −0.534 | −0.270 | −0.067 | 0.228 |
| **EUR** | 0.243 | −0.265 | −0.308 | 0.688 | −0.119 | 0.490 | 0.127 | −0.179 |
| **GBP** | 0.083 | −0.471 | 0.579 | −0.104 | 0.552 | 0.296 | −0.046 | −0.176 |
| **JPY** | 0.353 | 0.741 | 0.200 | 0.325 | 0.397 | 0.009 | −0.145 | −0.055 |
| **NOK** | 0.472 | −0.194 | −0.190 | −0.147 | −0.099 | −0.334 | −0.527 | −0.532 |
| **SEK** | 0.427 | −0.283 | −0.238 | 0.093 | 0.382 | −0.472 | 0.324 | 0.446 |
| **Explained** | 61.26% | 26.49% | 7.26% | 2.80% | 0.93% | 0.53% | 0.39% | 0.34% |
| | | | | *Regression residuals* | | | | |
| **AUD** | 0.532 | 0.138 | 0.019 | −0.261 | 0.665 | −0.025 | −0.368 | −0.227 |
| **CAD** | 0.276 | −0.057 | −0.175 | −0.271 | 0.248 | 0.057 | 0.657 | 0.566 |
| **CHF** | 0.177 | −0.243 | 0.662 | 0.273 | 0.070 | −0.594 | 0.052 | 0.193 |
| **EUR** | 0.178 | −0.291 | −0.430 | 0.732 | 0.248 | −0.004 | 0.205 | −0.244 |
| **GBP** | −0.086 | −0.440 | 0.489 | 0.024 | 0.195 | 0.714 | 0.073 | −0.082 |
| **JPY** | 0.558 | 0.539 | 0.243 | 0.289 | −0.372 | 0.303 | 0.154 | −0.050 |
| **NOK** | 0.369 | −0.451 | −0.060 | −0.399 | −0.409 | −0.148 | 0.229 | −0.506 |
| **SEK** | 0.351 | −0.384 | −0.209 | 0.068 | −0.295 | 0.144 | −0.555 | 0.516 |
| **Explained** | 65.70% | 16.33% | 10.65% | 3.10% | 2.12% | 1.20% | 0.54% | 0.34% |

Table IA.3: $R^2$ of different variable combinations

This table reports the $R^2$ (in %) from currency excess return forecasting regressions (with currency fixed effects) using all possible univariate, bivariate, 3-variate and 4-variate combinations of the quanto-implied risk premium (QRP), the interest rate differential (IRD), the average interest rate differential ($\overline{\text{IRD}}$), and the real exchange rate (RER).

| | univariate | bivariate | 3-variate | 4-variate |
|---|---|---|---|---|
| QRP | 22.03 | | | |
| RER | 7.97 | | | |
| IRD | 2.77 | | | |
| $\overline{\text{IRD}}$ | 2.06 | | | |
| QRP, RER | | 35.40 | | |
| $\overline{\text{IRD}}$, RER | | 34.47 | | |
| IRD, RER | | 28.22 | | |
| QRP, $\overline{\text{IRD}}$ | | 22.77 | | |
| QRP, IRD | | 22.60 | | |
| IRD, $\overline{\text{IRD}}$ | | 2.79 | | |
| QRP, $\overline{\text{IRD}}$, RER | | | 43.56 | |
| QRP, IRD, RER | | | 39.89 | |
| IRD, $\overline{\text{IRD}}$, RER | | | 36.77 | |
| QRP, IRD, $\overline{\text{IRD}}$ | | | 22.80 | |
| QRP, IRD, $\overline{\text{IRD}}$, RER | | | | 44.09 |

## Table IA.4: Quantos and the real exchange rate

This Table presents results from currency excess return forecasting regressions that extend the baseline results in Table 4 by adding the log real exchange rate to the regressors on the right-hand side. Following Dahlquist and Penasse (2017), we compute the log real exchange rate as $\text{RER}_{i,t} = \log\left(e_{i,t}\frac{P_{i,t}}{P_{\$,t}}\right)$, where $P_{i,t}$ and $P_{\$,t}$ are consumer price indices for country $i$ and the US, respectively, obtained from the OECD.

$$\frac{e_{i,t+1}}{e_{i,t}} - \frac{R^{\$}_{f,t}}{R^{i}_{f,t}} = \alpha_i + \beta\,\text{QRP}_{i,t} + \gamma\,\text{IRD}_{i,t} + \zeta\,\text{RER}_{i,t} + \varepsilon_{i,t+1} \tag{IA.D.1}$$

$$\frac{e_{i,t+1}}{e_{i,t}} - \frac{R^{\$}_{f,t}}{R^{i}_{f,t}} = \alpha_i + \beta\,\text{QRP}_{i,t} + \zeta\,\text{RER}_{i,t} + \varepsilon_{i,t+1} \tag{IA.D.2}$$

$$\frac{e_{i,t+1}}{e_{i,t}} - \frac{R^{\$}_{f,t}}{R^{i}_{f,t}} = \alpha_i + \gamma\,\text{IRD}_{i,t} + \zeta\,\text{RER}_{i,t} + \varepsilon_{i,t+1} \tag{IA.D.3}$$

$$\frac{e_{i,t+1}}{e_{i,t}} - \frac{R^{\$}_{f,t}}{R^{i}_{f,t}} = \alpha_i + \zeta\,\text{RER}_{i,t} + \varepsilon_{i,t+1} \tag{IA.D.4}$$

The two panels report coefficient estimates for each pooled and fixed effects regression, respectively, with standard errors (computed using a nonparametric block bootstrap) in parentheses. See Section 2.6 for more detail.

| *Panel regressions with currency fixed effects* | | | | |
|---|---|---|---|---|
| Regression | (IA.D.1) | (IA.D.2) | (IA.D.3) | (IA.D.4) |
| QRP, $\beta$ | 4.292 | 5.654 | | |
| | (1.843) | (1.402) | | |
| IRD, $\gamma$ | -2.624 | | -4.791 | |
| | (1.547) | | (1.242) | |
| RER, $\zeta$ | -0.616 | -0.413 | -0.729 | -0.314 |
| | (0.205) | (0.136) | (0.201) | (0.162) |
| $R^2$ | 39.89 | 35.40 | 28.22 | 7.97 |

Table IA.5: Separate return forecasting regressions using QRP and IRD predictors

This table reports the results of running regressions (20), (21), (22), and (24) separately for each currency at the 24-month horizon, and at 6- and 12-month horizons for the euro. We report the OLS estimates along with Hansen–Hodrick standard errors. $R^2$ are reported in %.

| Currency | AUD | CAD | CHF | DKK | EUR | EUR | EUR | GBP | JPY | KRW | NOK | PLN | SEK |
|---|---|---|---|---|---|---|---|---|---|---|---|---|---|
| Horizon | 24m | 24m | 24m | 24m | 6m | 12m | 24m | 24m | 24m | 24m | 24m | 24m | 24m |
| *Panel A: Regression (20)*: $e_{i,t+1}/e_{i,t} - R^{\$}_{f,t}/R^{i}_{f,t} = \alpha + \beta\,\mathrm{QRP}_{i,t} + \varepsilon_{i,t+1}$ | | | | | | | | | | | | | |
| $\alpha$ (p.a.) | −0.062 | −0.085 | −0.003 | −0.052 | −0.040 | −0.071 | −0.060 | −0.086 | −0.012 | −0.068 | −0.180 | −0.065 | −0.106 |
| | (0.071) | (0.042) | (0.038) | (0.022) | (0.056) | (0.052) | (0.030) | (0.031) | (0.090) | (0.034) | (0.061) | (0.026) | (0.048) |
| $\beta$ | 3.258 | 4.754 | −1.657 | 4.125 | 3.702 | 6.361 | 4.148 | 9.217 | 4.750 | 4.227 | 11.860 | 3.580 | 5.930 |
| | (3.991) | (3.546) | (6.903) | (1.723) | (6.263) | (5.527) | (3.367) | (3.791) | (10.959) | (1.757) | (4.698) | (0.956) | (3.316) |
| $R^2$ | 12.15 | 25.39 | 0.60 | 17.42 | 3.17 | 17.98 | 25.93 | 57.48 | 4.06 | 46.59 | 49.96 | 33.01 | 38.00 |
| *Panel B: Regression (21)*: $e_{i,t+1}/e_{i,t} - R^{\$}_{f,t}/R^{i}_{f,t} = \alpha + \gamma\,\mathrm{IRD}_{i,t} + \varepsilon_{i,t+1}$ | | | | | | | | | | | | | |
| $\alpha$ (p.a.) | −0.091 | −0.006 | 0.001 | 0.014 | −0.015 | −0.019 | −0.034 | −0.043 | −0.152 | 0.007 | −0.091 | 0.005 | −0.042 |
| | (0.084) | (0.030) | (0.027) | (0.023) | (0.083) | (0.040) | (0.025) | (0.034) | (0.046) | (0.034) | (0.065) | (0.045) | (0.035) |
| $\gamma$ | −2.859 | 4.135 | −2.246 | 2.147 | 2.626 | 1.869 | −1.439 | −5.564 | 25.539 | 0.312 | −3.310 | −0.118 | −1.765 |
| | (2.743) | (3.543) | (3.067) | (2.036) | (7.375) | (6.349) | (3.255) | (6.779) | (8.318) | (3.011) | (3.698) | (1.211) | (2.730) |
| $R^2$ | 19.82 | 12.30 | 7.33 | 13.77 | 1.23 | 1.31 | 3.90 | 6.93 | 57.26 | 0.14 | 14.39 | 0.09 | 7.28 |
| *Panel C: Regression (22)*: $e_{i,t+1}/e_{i,t} - 1 = \alpha + \beta\,\mathrm{QRP}_{i,t} + \gamma\,\mathrm{IRD}_{i,t} + \varepsilon_{i,t+1}$ | | | | | | | | | | | | | |
| $\alpha$ (p.a.) | −0.093 | −0.055 | 0.010 | −0.041 | −0.055 | −0.092 | −0.078 | −0.082 | −0.165 | −0.063 | −0.185 | −0.041 | −0.117 |
| | (0.087) | (0.044) | (0.035) | (0.021) | (0.053) | (0.043) | (0.027) | (0.033) | (0.079) | (0.046) | (0.070) | (0.032) | (0.043) |
| $\beta$ | 0.698 | 5.291 | −1.698 | 5.252 | 10.008 | 12.916 | 7.321 | 9.760 | −1.348 | 4.241 | 11.230 | 4.736 | 7.895 |
| | (3.130) | (2.984) | (6.621) | (1.260) | (7.198) | (4.771) | (2.895) | (3.519) | (7.485) | (1.719) | (3.491) | (0.848) | (2.552) |
| $\gamma$ | −1.525 | 6.019 | −1.250 | 3.857 | 11.447 | 11.992 | 4.651 | 3.094 | 27.182 | 1.514 | 0.253 | 2.419 | 2.938 |
| | (2.429) | (2.637) | (3.050) | (1.671) | (8.450) | (4.880) | (2.175) | (3.124) | (8.344) | (2.149) | (2.402) | (1.003) | (1.683) |
| $R^2$ | 9.79 | 46.74 | 3.04 | 48.62 | 14.42 | 45.19 | 33.51 | 57.29 | 59.41 | 48.22 | 46.61 | 45.28 | 39.00 |
| *Panel D: Regression (24)*: $e_{i,t+1}/e_{i,t} - 1 = \alpha + \gamma\,\mathrm{IRD}_{i,t} + \varepsilon_{i,t+1}$ | | | | | | | | | | | | | |
| $\alpha$ (p.a.) | −0.091 | −0.006 | 0.001 | 0.014 | −0.007 | −0.019 | −0.034 | −0.043 | −0.152 | 0.007 | −0.091 | 0.005 | −0.042 |
| | (0.084) | (0.030) | (0.027) | (0.023) | (0.041) | (0.040) | (0.025) | (0.034) | (0.046) | (0.034) | (0.065) | (0.045) | (0.035) |
| $\gamma$ | −1.859 | 5.135 | −1.246 | 3.147 | 3.626 | 2.869 | −0.439 | −4.564 | 26.539 | 1.312 | −2.310 | 0.882 | −0.765 |
| | (2.743) | (3.543) | (3.067) | (2.036) | (7.375) | (6.349) | (3.255) | (6.779) | (8.318) | (3.011) | (3.698) | (1.211) | (2.730) |
| $R^2$ | 9.47 | 17.78 | 2.38 | 25.54 | 2.32 | 3.03 | 0.38 | 4.77 | 59.13 | 2.48 | 7.57 | 4.79 | 1.45 |

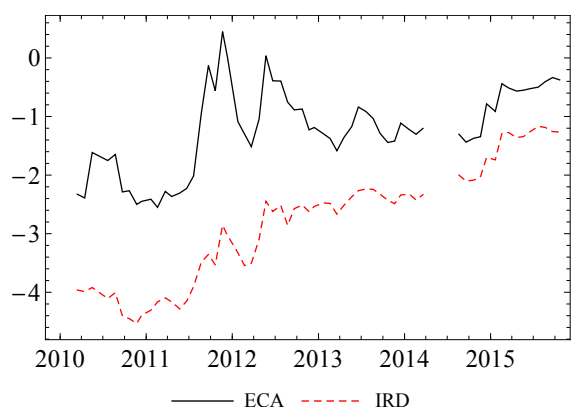


(a) AUD

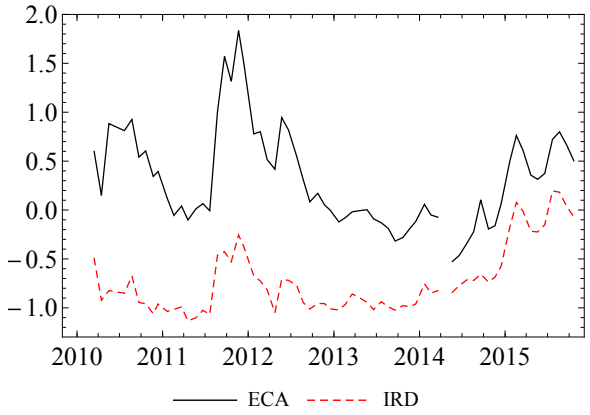


(b) CAD

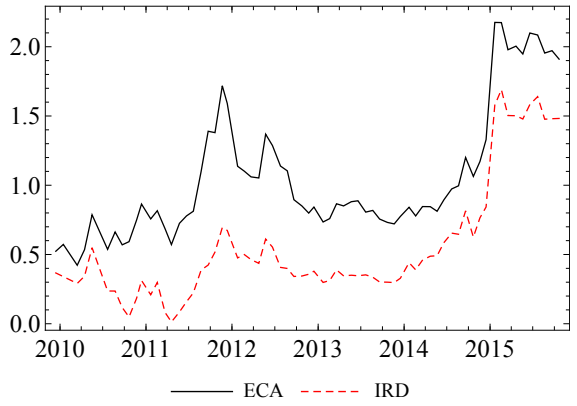


(c) CHF

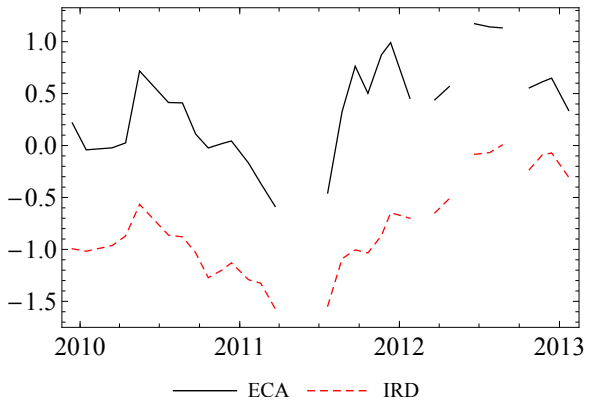


(d) DKK

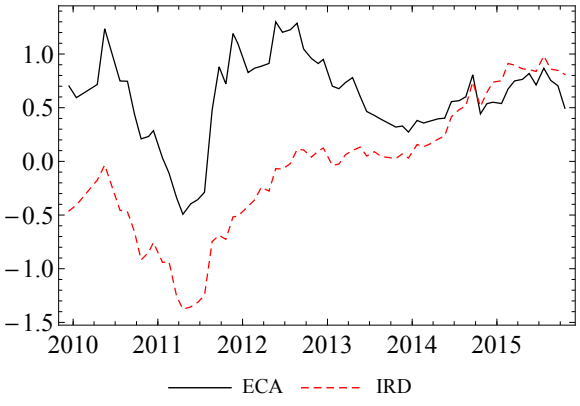


(e) EUR

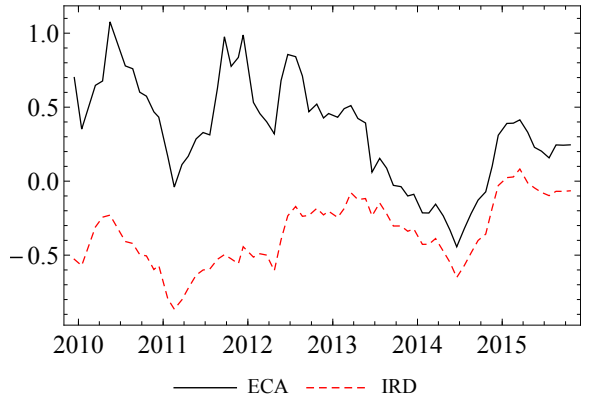


(f) GBP

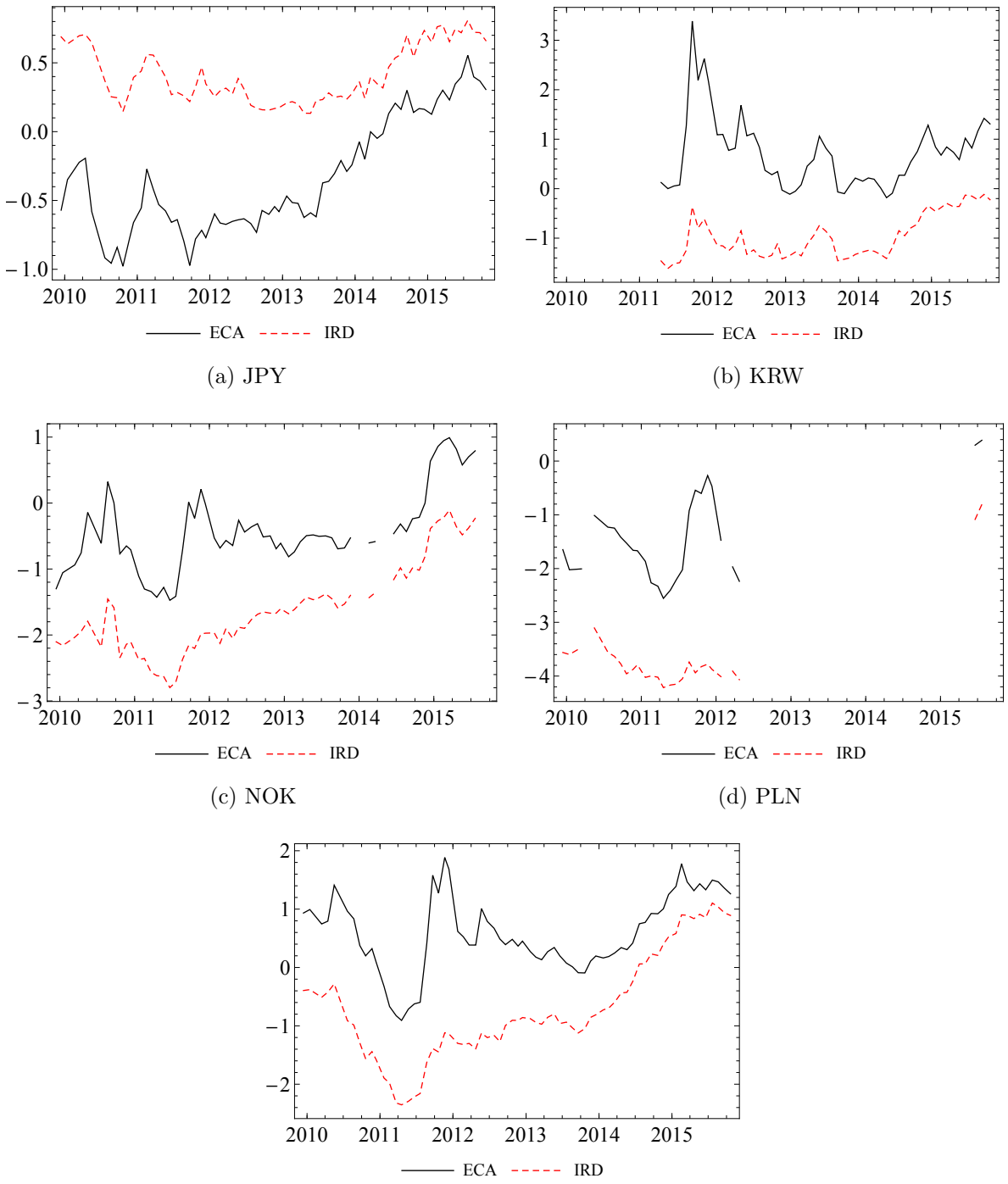


(a) JPY

(b) KRW

(c) NOK

(d) PLN

(e) SEK

Figure IA.6: Time series of annualized expected currency appreciation implied by the quanto theory (ECA) and by UIP (IRD).

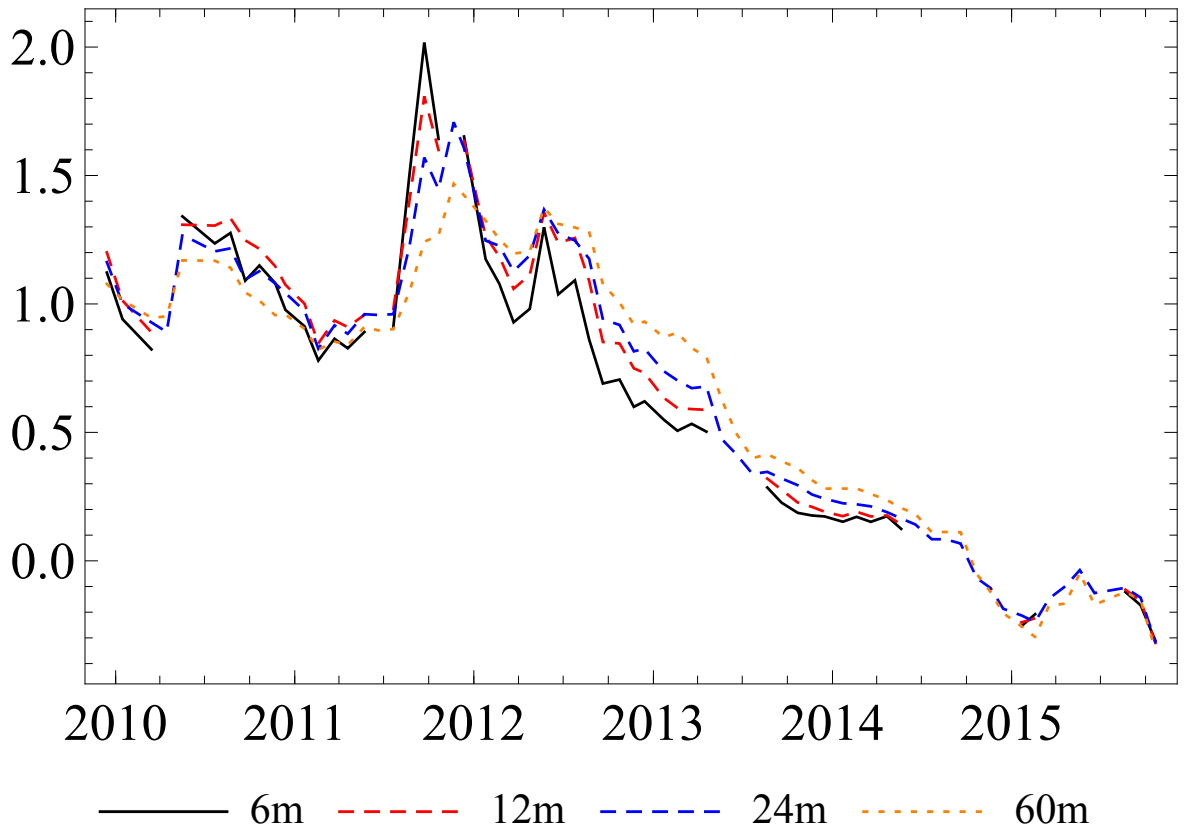


Figure IA.7: Term structure of the euro-dollar risk premium, as measured by QRP, in the time series for horizons of 6, 12, 24, and 60 months.

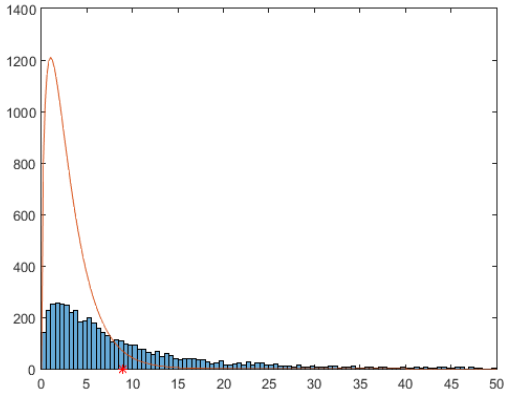


(a) Pooled, $H_0^1$

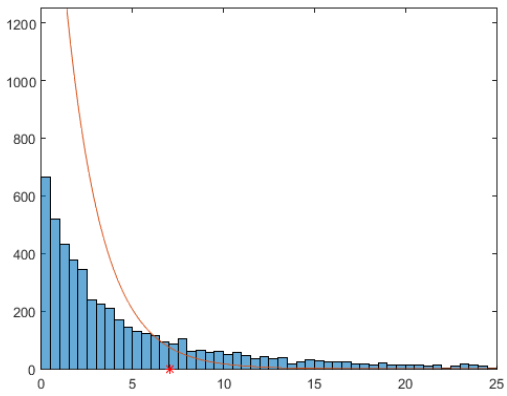


(b) Fixed effects, $H_0^2$

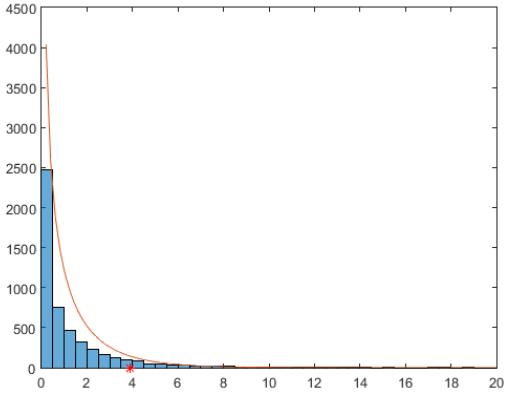


(c) Pooled, $H_0^3$

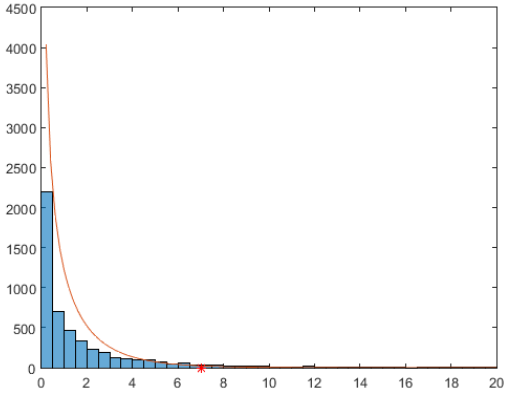


(d) Fixed effects, $H_0^3$

Figure IA.8: Histogram of the small-sample distributions of the test statistics for various hypotheses on regression (22). The asymptotic distribution is shown as a solid line. Asterisks indicate the test statistics for the original sample.

# References

**Colacito, Riccardo, and Mariano M. Croce.** 2011. "Risks for the Long Run and the Real Exchange Rate." *Journal of Political Economy*, 119(1): 153–182.

**Dahlquist, Magnus, and Julien Penasse.** 2017. "The Missing Risk Premium in Exchange Rates." *Working Paper*.

**Jordà, Òscar, and Alan M. Taylor.** 2012. "The Carry Trade and Fundamentals: Nothing to Fear but FEER itself." *Journal of International Economics*, 88: 74–90.